COVERING WITH CHITOSAN AND HYALURONIC ACID SHELLS OF IRON BASED NANOPARTICLES OBTAINED BY LASER PYROLYSIS FOR MEDICAL APPLICATIONS

Anca Daniela BĂDOI[1*], Iulia BĂRBUȚ[2], Bogdan BUTOI[3], Octavian DĂNILĂ[4], Mihai GANCIU[5], Cătălin LUCULESCU[6], Ion MORJAN[7], Claudiu FLEACĂ[8], Florian DUMITRACHE[9], Lavinia GAVRILĂ[10], Eugenia VASILE[11], Natalia MIHĂILESCU[12], Ana CUCU[13], Ion CIUCĂ[14]

Nanocomposite materials obtained by laser pyrolysis are very popular lately in biological applications at cellular level, but the major issue for these nanoparticles is their dispersion and functionalization. In this article, we describe the stabilization and functionalization of iron based magnetic nanoparticles using two different biopolymeric materials, namely chitosan and hyaluronic acid. We have obtained the iron oxide nanoparticles by laser pyrolysis technique, (maghemite phase) with precise size control and narrow size distributions. The nanoparticles were dispersed in water with chitosan and hyaluronic acid and were analyzed with TEM, DLS and FTIR. This progress, together with the availability of suitable bio-compatible coverage, are both of crucial importance, as premises for their biomedical applications.

Keywords: magnetic, nanoparticles, chitosan, hyaluronic acid, laser, pyrolysis

[1*] National Institute for Lasers, Plasma and Radiation Physics, Măgurele, Romania, e-mail: bad_anca20@yahoo.com
[2] National Institute for Lasers, Plasma and Radiation Physics, Măgurele, Romania
[3] National Institute for Lasers, Plasma and Radiation Physics, Măgurele, Romania
[4] Physics Department, Faculty of Applied Sciences, University POLITEHNICA of Bucharest and National Institute for Lasers, Plasma and Radiation Physics, Măgurele, Romania
[5] National Institute for Lasers, Plasma and Radiation Physics, Măgurele, Romania
[6] National Institute for Lasers, Plasma and Radiation Physics, Măgurele, Romania
[7] National Institute for Lasers, Plasma and Radiation Physics, Măgurele, Romania
[8] National Institute for Lasers, Plasma and Radiation Physics, Măgurele and , Appl. Sci Faculty, Physics Dept., University POLITEHNICA of Bucharest, Romania
[9] National Institute for Lasers, Plasma and Radiation Physics, Măgurele and Appl. Sci Faculty, Physics Dept., University POLITEHNICA of Bucharest
[10] National Institute for Lasers, Plasma and Radiation Physics, Măgurele, Romania
[11] University POLITEHNICA of Bucharest, Romania
[12] National Institute for Lasers, Plasma and Radiation Physics, Măgurele, Romania
[13] University of Bucharest, Faculty of Physics, Res Ctr 3Nano SAE, Bucharest, Romania
[14] Prof., Faculty of Materials Science and Engineering, University POLITEHNICA of Bucharest, Romania

1. Introduction

Nanocomposite materials with functional biocompatible or bioactive substances forming a shell and magnetic cores deliverable at cellular level have been designed for many biomedical applications such as: drug delivery [1], hyperthermia [2], magnetic resonance imaging enhancement, fluorescent probes [3], enzymes/proteins absorption [4], antibacterial coatings [5], protein separation [6] etc. The major issue for such nanocomposites is to optimize a strong magnetic response with high stability in aqueous-based media and to improve the functional capacity of the external shell. These nanocoatings can be composed from polymers with high stability in aqueous media, who also have the role to reduce the undesired aggregation phenomena. Unfortunately there is a large category of useful magnetic nanoparticles with very low stability in aqueous solutions or relevant toxicity [7]. In these cases magnetic dispersions based on magnetic nanoparticles imply coating and functionalized procedures [8]. For medical applications, the particles must have combined properties of high magnetic saturation, biocompatibility and interactive functions at the surface. The surfaces of these particles could be modified through the creation of organic polymer (e.g. chitosan) thin layer, suitable for further functionalization by the attachment of various bioactive molecules [9]. In the last decade, the increased number of investigations with several types of iron oxides have been carried out in the field of nanosized single–domain magnetic particles (mostly maghemite, γ-Fe_2O_3, or magnetite, Fe_3O_4 [10], of about 5–20 nm in diameter), among which magnetite is a very promising candidate since it's biocompatibility has already proven [11]. Yet, in certain specific conditions, the magnetite phase is not stable and can release Fe^{2+} ions which generate toxic hydroxyl radicals via Fenton process [12]. The object of this article is to synthesize by laser pyrolysis the uniform size of the maghemite nanoparticles (Fe_2O_3), which will be functionalized with chitosan molecules and then covered with hyaluronic acid by the layer-by-layer method [13]. The hyaluronan-functionalized particles can be applied internally their introduction in the affected knee by injecting in sinovial liquid and being handled and controlled with an external knee orthosis [14] with a magnet [15]. Also hyaluronic acid has been extensively studied and found to be suitable for a wide range of tissue engineering applications [16]. A compelling solution is chitosan, which is a natural linear cationic polyelectrolyte having high hydrophylicity and biocompatibility (is non toxic for the human body) used in various applications such as for non-viral gene delivery sistem, in agriculture, food, medicine, biotechnology, textiles, polymer and water treatment [17,18].

Medical applications need a special surface covering of a magnetic particles, wich has to be not only non-toxic and biocompatible but also to allow a target delivery nanoparticles. Thus, most research in this area have been made to

improve the biocompatibility of materials, but only a few scientific research and development demonstrated an improving of the quality of magnetic particles, regarding their size distribution, shape and their surface in addition to characterize them in order to get a protocol for the quality control of these particles [19][8]. In this paper we wish to report the development of a procedure to obtained well stabilized aqueous dispersions containing laser pyrolysis synthesized iron oxide nanoparticles on a 'layer-by-layer' structure, covered first with chitosan and secondly with hyaluronic acid and the relevant investigations with TEM, DLS and FTIR. We add in the Introduction part the phrase "Our original contribution compared with existing research which there are obtained by coprecipitation and other methods [20] is that we obtain smaller and biocompatible magnetic nanoparticles by laser pyrolysis in our laboratory"

2. Experimental procedure

In our paper, the iron based oxide nanoparticles were obtained by laser pyrolysis, a technique based on infrared photochemistry [21,22]. The focused continuous wave CW CO_2 laser radiation (maximum output power 120 W, λ = 10.6 μm) was orthogonally crossed with the reactant gas stream which was admitted to the center of the reaction cell through a two-nozzle injection system.The presentation will be clear and concise and the symbols used therein will be specified in a symbol list (if necessary). In the paper it will be used the measurement units International System. In the paper, there will be no apparatus or installation descriptions.

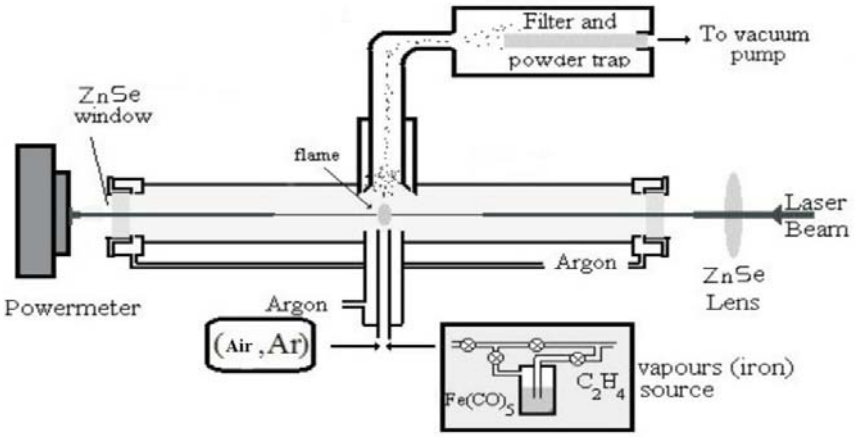

Fig. 1. Experimental set-up for the iron oxide creations

Thus, the reactive flow ($Fe(CO)_5$ vapors entrained by C_2H_4) was introduced through the central inner tube while an argon flow emerged in the reaction cell through the outer concentric tube. The reactive mixture was confined

to the flow axis using an innert Ar stream. In order to prevent the unwanted deposition of powders on the ZnSe windows, they were consequently flushed with separate Ar streams. During the experiment, the pressure in the reactor was maintained constant by leveling out the incoming and extracted flows using a vacuum pump and a feed-back regulated throttle valve. Since the $Fe(CO)_5$ molecule does not absorb in the 10.6 μm region, C_2H_4 was used as sensitizer due to the presence in their IR spectrum of an intense absorption band in this region. The system temperature increases by collision-induced processes with the excited gas component, resulting the decomposition of the organometallic precursor followed by rapid oxidation of the freshly-formed iron clusters in the presence of the oxygen molecules [23]. For the raw nanoparticles the main experimental parameters of synthesis are presented in the table 1.

Table 1

Experimental parameters for the raw nanoparticles synthesis

Sample	Laser power/Ar [W]	Pressure [mbar]	$D_{C2H4\ carriyng\ Fe(CO)5\ vapors}$ [sccm]	D air [sccm]	D_{Ar} [sccm]
Fe_2O_3	35	300	100	100	2000

The laser pyrolysis-obtained powder collected on a porous filter has a brown colour, specific to maghemite iron oxide. For the preparation of the initial oxidic nanoparticle suspension we used the following ingredients: 0.25 g of powder, 35 ml of distilled water, 0.72 ml of concentrated aqueous ammonia solution. The resulting solution was constructed as to exhibit a basic pH. Dispersion of the nanoparticles in the solution was obtained by means of ultra-sound mixing (UIP1000hd Ultrasonic Homogenizer- Hielscher-USA Instruments) endowed with a 2.5 cm diameter titanium sonotrode. The nanoparticle's final concentration in the resulted aqueous dispersion was 0.71 g/l. A quantity of 20 ml from this suspension were mixed first with 2 ml of pure acetic acid and then with 0,4 g of chitosan. The role of the acetic acid was to ensure an acidic pH which is required for chitosan-magnetic particle binding. The suspension was placed again under ultrasonic, finally obtaining a brown dispersion. After this procedure, 10 ml from the chitosan-covered nanoparticle suspension were mixed with 1 ml of solution containing 0.02 g hyaluronic acid dissolved in distilled water. A similar mixture was obtained from the uncoated iron oxide nanoparticle suspension. The resulted aqueous suspensions were also homogenized with the sonotrode on the ice bath. We have obtained 3 different liquid-based brown samples: one with magnetic nanoparticles dispersed in distilled water with ammonia, the second with magnetic nanoparticles coated with chitosan and the third containing magnetic nanoparticles coated with chitosan and hyaluronic acid.

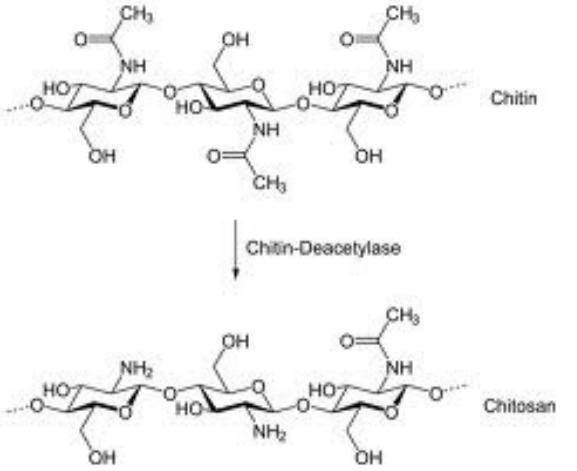

a)

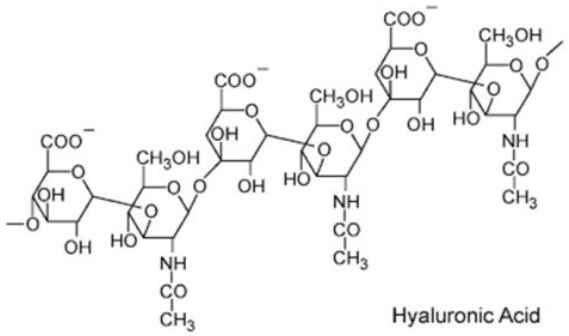

b)

Fig. 2. The chitosan (a) and hyaluronic acid (b) chemical formula

The obtained dispersions were analyzed by DLS (Dynamic Light Scattering) technique, with an Zetasizer-Malvern Instruments Inc (working in the 0.6-6000 nm range), together their Zeta PotenȚial, where a 1/100 dilution with distilled water was used in order to obtained a transparent dispersion. The chemical bond types of the dried powders were evaluated by FTIR (Fourier Transform Infrared Spectroscopy), using a Shimadzu 8400S FTIR Spectroscopy using a mixture 1:100 with KBr powder. The water-diluted samples from the three suspensions were pipetted copper grids covered with amorphous carbon and then introduced in a Tecnai F30 G2 Transmission Electron Microscope (TEM) working up to 300 kV, in order to evaluate the morphology of the (un)coated

magnetic nanoparticles. The magnetic measurements were performed at room temperature using a Vibrating Sample Magnetometer DMS 880. The size, morphology and elemental composition of the as synthesized nanoparticles were studied by X-ray diffraction (XRD) using a X-ray Diffractometer X'Pert Pro MPD and Energy-Dispersive X-ray spectroscopy (EDS) using a EDAX Inc., respectively.

3. Results and discussions

For a semi-quantitative evaluation of elemental composition EDS analysis were performed. By averaging the values from three measurements the following composition was established: 9.85 at.% C, 54.12 at.% O and 36.03 at.% Fe resulting the following chemical formula: $Fe_2O_{3+0.04}$ that it means very close of maghemite/hematite stoichiometry. The XRD patterns of the as synthesized iron oxide powder along with the most relevant Miller indices of the identified crystalline phase: γFe_2O_3 are shown în Fig.3. Other peaks with relative intensity less than 10% from absolute diffraction maximum (plane- <311>) are only assigned on the diffraction image. The main peaks assigned with (311), (400) and (440) planes (see Fig. 3) were fitted with pseudo - Voigt function and then the maximum peak position (2θ) and the FWHM parameters were established. Based on FWHM and Debye-Scherrer equation the mean crystallite sizes were determined. These values are presented in table 2. The spacing values extracted from major diffraction peaks with their 2θ positions are used for lattice constant evaluation, assuming a cubic structure. The mean value for lattice constant a_{mean}= 8.299 Å are lower than all literature-based values of maghemite and magnetite, where the most common phases are: maghemite-C /syn from spatial group: P4132 (213) and the constant lattice a= 8.352 Å (JCPDS file: 039-1346) or magnetite syn from spatial group: Fd-3m (227) and constant lattice a=8.397 Å (JCPDS file: 077-1545). Taking these values in account, the nanometric size of around 3 nm of the powder characterized and the elemental composition we may conclude that the nanopowders has a highly disordered maghemite structure.

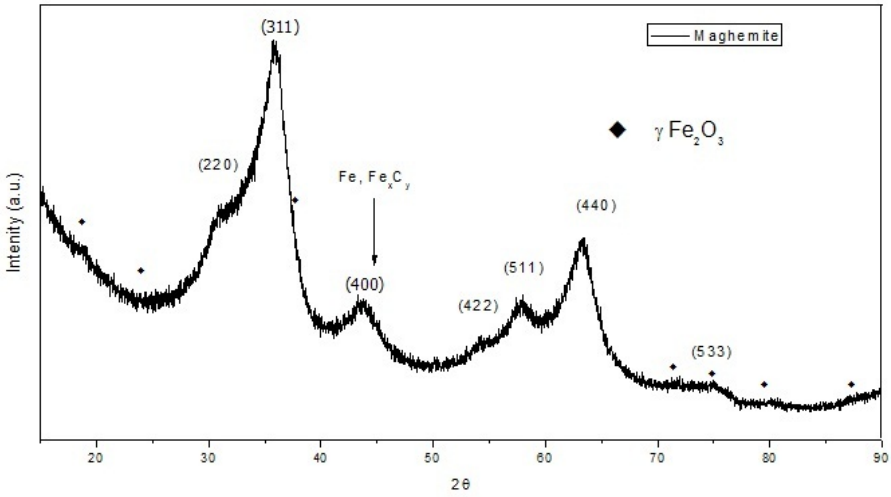

Fig. 3. XRD pattern of the as synthesized iron oxide nanoparticle

Table 2

2θ peak positions, crystallite sizes and lattice constant evaluated from the main diffraction crystalline planes

plane	2θ dgr	d_{mean} (nm)	a (Å)
(311)	43.85	2.98	8.305
(400)	63.24	3.31	8.254
(440)	35.83	3.53	8.31

The measurements of the virgin curve at room temperature were performed and the main parameter was extracted and shown in Table 3. The low coercive field values in addition with a significantly high saturation magnetization may be an indication of a dominant superparamagnetic feature of the as synthesized nanoparticle. Moreover, the decreased values of coercive field for all measured dispersions in comparison with the value related to as synthesized nanoparticle may be explained because only a few big particles with single magnetic domain size remained during the stabilization and dispensation processes.

Table 3

Magnetic parameters extracted from magnetic virgin curve measured at room temperature

Sample	Powder Concentration (g/l)	Coercitive field (Oe)	Saturation magnetisation		Magnetic permeability at H=0 Emu/Oe
			Specific (emu/g)	Volumic (Gs)	
Maghemite as synthesized	-	1784	15 (emu/g)		$2.35*10^{-4}$
Raw maghemite (dispersion)	0.1	682.6		0.134	$5.63*10^{-7}$
Maghemite+C Covered (dispersion)	0.1	462.9		0.032	$1.87*10^{-7}$
Maghemite+C+HA Covered (dispersion)	0.1	352.5		0.030	$1.85*10^{-7}$

Dimensional analysis of the particles in the obtained dispersions is particularly important for final evaluation of a colloidal system. Due to the gas phase-technique used for the synthesis our nanoparticles forms aggregates which themselves undergo agglomeration in different degrees in the concentrated water suspensions.

Table 4

The DLS parameters

Dispersion	Main peaks size (nm)	Average size (nm)	Zeta Potential (mV)
Raw	129 → 92 % 41,86 → 8 %	116,6	-30,3
Chitosan-coated	163,7 → 91,2 % 33,65 → 8,8 %	144,7	46,8
Chitosan+Hyaluronic Acid coated	124,2 → 100 %	122,1	44,9

One can observe a bimodal particle size distribution with a small peak under 50 nm from Figs. 4 and 5, the main peak being centered at a value higher than 125 nm.

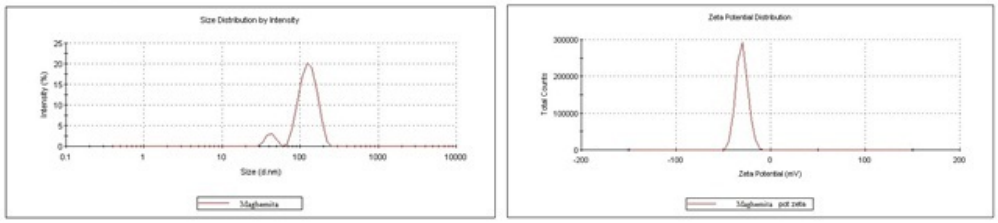

Fig. 4. Size and zeta potential of maghemite raw nanoparticles sample

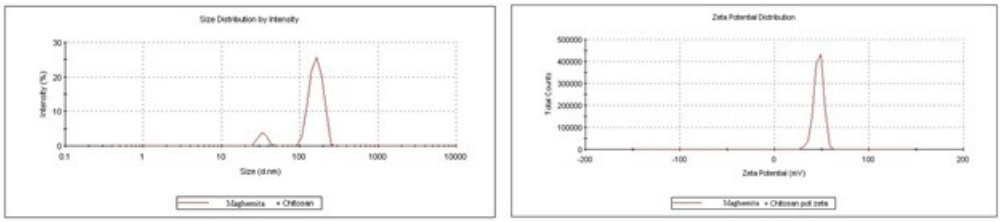

Fig. 5. Size and zeta potential of maghemite+chitosan nanoparticles sample

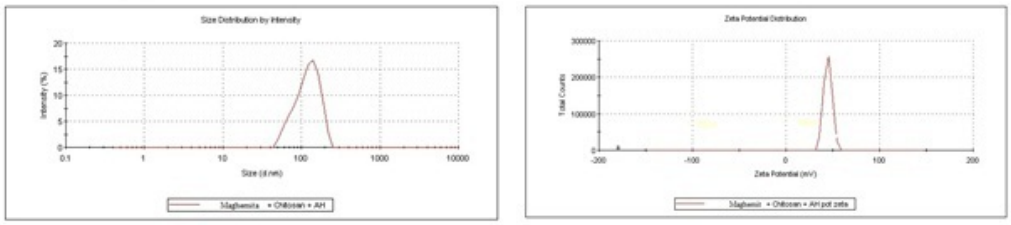

Fig. 6. Size and zeta potential of maghemite+chitosan+hyaluronic acid nanoparticles sample

For the chitosan+hyaluronic acid covered nanoparticles (Fig. 6) we observed a single peak centered at 124 nm, yet with a much broader distribution of sizes (from ~35-240 nm). The increase of the mean hydrodynamic diameter from the raw nanoparticles to those coated with chitosan can be explained by the covering of the negative surface of maghemite with the cationic chitosan. The chitosan + hyaluronic acid covered maghemite particles suspension seems to have a smaller mean size than those coated only with chitosan wich can be explained (after corroborating with their wider size distribution) by the partially fusion of smaller chitosan coated nanoparticles trough a common hyaluronic acid layer composed form very long chains (up to 10 μm in the unfolded conformation). The raw nanoparticle suspension - being obtained in a basic medium (due to ammonia presence) have a relatively high negative zeta potential value (-30.3 mV, see table 4) provided by the reaction of hydroxy (HO^-) anions with iron oxide surface which can be schematized as follows:

$$NH_3 + H_2O \rightarrow NH_4^+ + HO^- \quad (1)$$

$$Fe_{surface} - OH + HO^- \rightarrow Fe_{surface} - O^- + H_2O \quad (2)$$

After introducing the chitosan, the zeta potential value has changed the sign and become positive due to the neutralization of initial negative charges of oxide surface with the positive charges beared by the partially hydrolyzed polymer in the acidic medium.

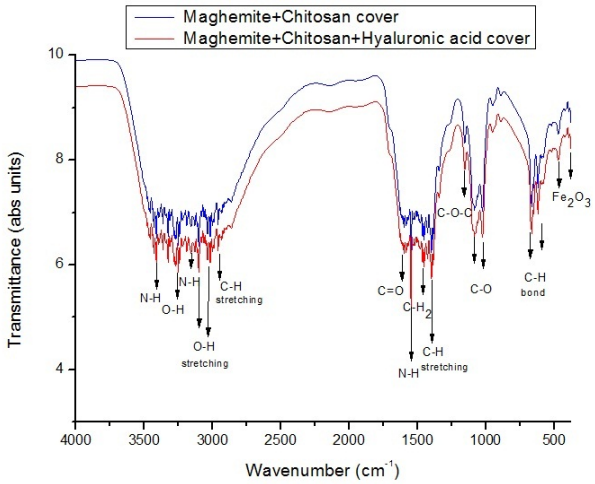

Fig. 7. FTIR Spectrum of covered maghemite nanoparticles: maghemite+Chitosan and maghemite+Chitosan+Hyaluronic Acid

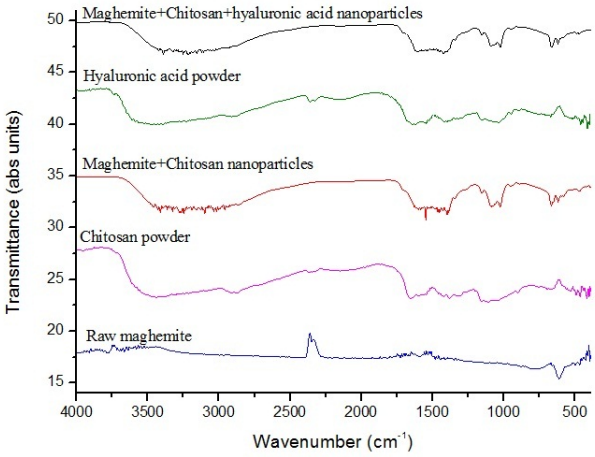

Fig. 8. FTIR Spectrum of the three types of nanoparticles spectra overlapped with the standard powders spectra

The region between 3000 cm^{-1} and 3500 cm^{-1} shows the stretching of OH groups. This band is broad because of the presence of hydrogen bonds and it is

observed for the samples with chitosan nanoparticles covered but also at hyaluronic acid cover nanoparticles, because both polymers have OH groups.

From the recorded overlapped IR spectra of both pure polymers, raw iron oxide nanoparticles and polymer coated nanoparticles, it can be concluded that the chitosan and hyaluronic acid were attached to the maghemite particles because the structural pattern of the both polymers were observed on the polyelectrolyte mono or double layers covered nanoparticles (Fig.8). The detailed FTIR spectra of the two nanocomposites (Fig. 7) reveals the presence of hydroxyl –OH groups from chitosan and hyaluronic acid and $–NH_2$ (only from chitosan) on the covered nanoparticles. The characteristic bands found at 3200 cm^{-1} and 3680 cm^{-1}, respectively, with their counterpart in the region 1790–1520 cm^{-1}, can be clearly seen in the spectra. The carbonyl signature vibration from the amide group (-$NHCOCH_3$) can be found in both hyaluronan and chitosan-coated particles (as non-deacetylated groups from the parent chitin polymer) around 1600-1604 cm^{-1}. Also, the C-O-C asymmetric stretching signature was found at 1153 cm^{-1} for both chitosan and chitosan+hyaluronic acid samples. This peak is attributed to the glycosidic bond and is found in all polysaccharides, being reported from cellulose at 1160 cm^{-1}[24]. The IR peaks of maghemite were observed in both samples in the 409-640 cm^{-1} zone (see Fig. 7, 8), similar with those reported by Veintemillas et all. in [25]. TEM images (see Fig. 9) confirm the presence of aggregates/ agglomerates detected also by DLS technique. Fig. 9 a) reveals clusters of individual quasispherical nanoparticles, each having diameters between 4-7 nm.

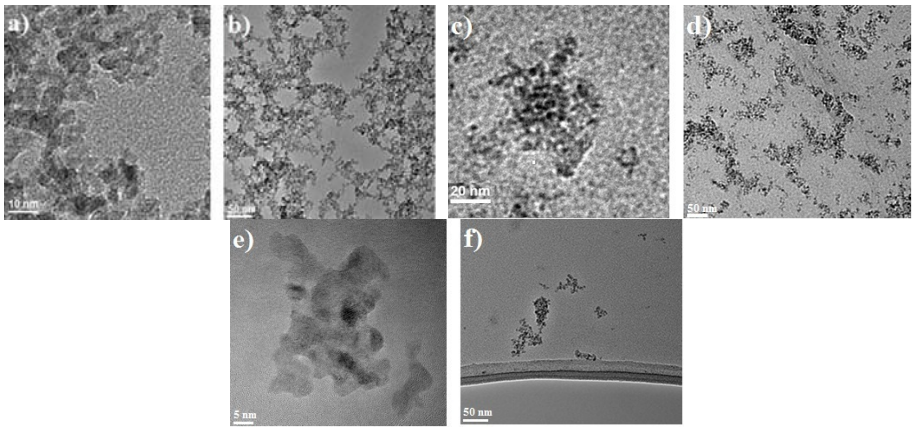

Fig. 9. Higher (left) and lower (right) resolution TEM images from the raw magnetic nanoparticles (a,b), chitosan coated (c,d) and chitosan+hyaluronic acid coated particles (e,f)

The particles forms fractal aggregates which assembles in web-like agglomerates as can be seen in Fig. 9 b). In Fig. 9 d) one can observe isolated nanoparticles aggregates with various sizes as resulted from the introduction of

the chitosan polymer. The higher resolution image from Fig. 9 c) confirms the polymer coated of an individual aggregate of iron oxide nanoparticles. Also an even higer resolution image presented in Fig. 9 e) shows a conformal layer which wraps a cluster of nanoparticles from the chitosan+hyaluronic acid coated maghemite sample. The sizes of the clusters (aggregates) visible in the Fig. 9 f) of the nanoparticles covered with both polymers match well with the sizes found by the DLS measurements (~35-240 nm) from the same samples.

4. Conclusions

It can be concluded that laser pyrolysis is a suitable technique for the obtaining spherical maghemite magnetic nanoparticles with small dimension. TEM and FTIR analysis confirm the direct deposition of successive layers of chitosan and hyaluronic acid on the surface of iron oxide nanoparticles. The coating allows a chitosan-based medium for advanced stabilization of the particle dispersion and strong elimination of agglomeration phenomena. Hyaluronic acid may have a complementary role to stabilize the positive particles coated with the first layer (chitosan). But excess hyaluronic acid can cause colloidal agglomeration phenomena. DLS analysis shows only a slight increased of the mean particle hydrodynamic diameters after polymer coating/ultrasonication processes. Zeta Potential measurements confirm the enhanced stability of the polymer coated nanoparticles due to polyelectrolyte nature of both chitosan and hyaluronic acid polymers. This kind of functionalization can have a broader field of applications: local drug delivery in the knee joint, hypertermia, magnetic resonance imaging enhancement, enzymes/proteins absorbtion or antibacterial coatings.

Acknowledgements

The work has been funded by the Sectoral Operational Programme Human Resources Development 2007-2013 of the Ministry of European Funds through the Financial Agreement Posdrus 159/1.5/S/134398.

REFERENCES

1. *F.A.Oyarzun-Ampuero, J.Brea, M.I.Loza, D.Torres, M.J.Alonso*, Chitosan–hyaluronic acid nanoparticles loaded with heparin for the treatment of asthma, International Journal of Pharmaceutics 381 (2009) 122–129
2. *S.Balasubramanian, A.R.Girija, Y.Nagaoka, S.Iwai, M.Suzuki, V.Kizhikkilot, Y.Yoshida, T.Maekawa, S.Dasappan*, Curcumin and 5-Fluorouracil-loaded, folate- and transferrin-decorated polymeric magnetic nanoformulation: a synergistic cancer therapeutic approach, accelerated by magnetic hyperthermia, International Journal of Nanomedicine vol 9,2014, 437–459

3. *C.Sanjai, S.Kothan, P.Gonil, S.Saesoo, W.Sajomsang*, Chitosan-triphosphate nanoparticles for encapsulation of super-paramagnetic iron oxide as an MRI contrast agent, Carbohydrate Polymers 104, 2014, 231–237
4. *N.Duceppe, M.Tabrizian*, Factors influencing the transfection efficiency of ultra low molecular weight chitosan/hyaluronic acid nanoparticles, Biomaterials 30, 2009, 2625–2631
5. *S.S.Behera, J.K.Patra, K.Pramanik, N.Panda, H.Thatoi*, Characterization and evaluation of antibacterial activities of chemically synthesized iron oxide nanoparticles, World Journal of Nano Science and Engineering, 2012, 2, 196-200
6. *C.Okoli, A.Fornara, J.Qin, M.S.Toprak, G.Dalhammar, M.Muhammed, G.K.Rajarao*, Characterization of superparamagnetic iron oxide nanoparticles and its application in protein purification, J Nanosci Nanotechnol. 2011 Nov;11(11):10201-6
7. *M.A.Maurer-Jones, Y.S.Lin, L.C.Haynes*, Functional assessment of metal oxide nanoparticle toxicity in immune cells, ACS Nano, 2010, 4 (6), pp 3363–3373
8. *M. Racuciu, D. Creanga, C. Nadejde*, Comparison among the physical properties of various suspensions of magnetite nanoparticles stabilized in water using different organic shells, U.P.B. Sci. Bull., Series A, Vol. 75, Iss. 3, 2013
9. *C.C.Berry, A.S.G.Curtis*, Functionalisation of magnetic nanoparticles for applications in biomedicine. J Phys D: Appl Phys, 2003, 36:R198–206
10. *C. Stan, C. P. Cristescu, M. Balasoiu, N. Perov, V. N. Duginov, T. N. Mamedov, L. Fetisov*, Investigations og a Fe_3O_4-ferofluid at different temperatures by means of magnetic measurements, U.P.B. Sci. Bull., Series A, Vol. 73, Iss. 3, 2011
11. *U.Schwertmann, R.M.Cornell*, Iron oxides in the laboratory: preparation and characterization, Weinheim, Cambridge: VCH; 1991
12. *N.Singh, G.J.S.Jenkins, E.Asadi, S.H.Doak*, Potenial toxicity ofiron oxide superparamagnetic Fe_2O_3 nanoparticles, Nano Reviews1 (2010) 5358-5373
13. *I.Morjan, F.Dumitrache, R.Alexandrescu, C.Fleaca, R.Birjega, C.R.Luculescu, I.Soare, E.Dutu, G.Filoti, V.Kuncser, G.Prodan, N.C.Popa, L.Vekas*, Laser synthesis of magnetic iron-carbon nanocomposites with size dependent properties, Advanced Powder Technology Volume 23, Issue 1,2012 Pages 88–96
14. *D.R.Kwon, G.Y.Park*, Intra-articular injections for the treatment of osteoarthritis: focus on the clinical use of several regimens, osteoarthritis – diagnosis, treatment and surgery, Chapter 4, , Published: March 2, 2012, 953-51-0168-0
15. *D.Laptoiu, I.Antoniac, A.Antoniac*, Testing the effect of permanent magnets on magnetic nanoparticles ferrofluid – targeted delivery inside knee articulation, Annals of DAAAM & Proceedings,Jan2011, p937
16. *M.Halbleib, S.Thomas, L.Claudio, von D.Heimburgc, H.Hauner,* Tissue engineering of white adipose tissue using hyaluronic acid-based scaffolds. I: in vitro differentia tion of human adipocyte precursor cells on scaffolds, Bio materials, 2003; 24: 3125–3132
17. *X.Wang, Y.Du, J.Luo, B.Lin, J.F.Kennedy*, Chitosan/organic rectorite nanocomposite films: Structure, characteristic and drug delivery behavior, Carbohydrate Polymers, 2007; 69: 41–49,

18. *J.M.Dang, K.W.Leong*, Natural polymers for gene delivery and tissue engineering, Advanced Drug Delivery Reviews, 2006; 58: 487– 499
19. *N.A.Frey, S.Peng, K.Cheng, S.Sun*, Magnetic nanoparticles: synthesis, functionalization, and applications in bioimaging and magnetic energy storage, Chem Soc Rev. 2009 Sep;38(9):2532-42,
20. *S.Laurent, D.Forge, M.Port, A.Roch, C.Robic, L.V.Elst, R.N.Muller*, Magnetic Iron Oxide Nanoparticles: Synthesis, Stabilization, Vectorization, Physicochemical Characterizations, and Biological Applications, Chemical Reviews 2008, 108, 2064–2110
21. *I.Morjan, R.Alexandrescu, I.Soare, F.Dumitrache, I.Sandu, I.Voicu, A.Crunteanu, E.Vasile, V.Ciupina, S.Martelli*, Nanoscale powders of different iron oxide phases prepared by continous laser irradiation of iron pentacarbonyl-containing gas precursors, (2003), Materials Science and Engineering C, 23 (1-2), pp. 211-216
22. *R.Alexandrescu, I.Morjan, I.Voicu, F.Dumitrache, L.Albu, I.Soare, G.Prodan*, Combining resonant/non-resonant processes: nano-meter-scale iron-based material preparation via the CO_2 laser pyrolysis, Applied Surface Science Volume: 248 Issue: 1-4, 2005, Pages: 138-146
23. *F.Dumitrache, I.Morjan, R.Alexandrescu, V.Ciupina , G.Prodan , I.Voicu, C.Fleaca, L.Albu, M.Savoiu, I.Sandu, E.Popovici, I.Soare*, Iron-Iron oxide core –shell nanoparticles synthesized by laser pyrolysis followed by superficial oxidation, Applied Surface Science Volume: 247 Issue: 1-4, 2005, Pages: 25-31
24. *K.Kavkler, A.Demsar*, Application of FTIR and Raman Spectroscopy to Qualitative Analysis of Structural Changes in Cellulosic Fibres, Tekstilec, 2012, letn. 55, št. 1, str. 19–31
25. *S.Veintemillas-Vertaguer, M.P.Morales, C.J.Serna*, Effect of the oxidation conditions on the maghemites produced by laser pyrolysis,Appl.Organomet.Chem. Volume 15, Issue 5, 2001, pages 365–372